Model-free Optimal Volt-VAR Control of Wind Farm Based on Data-driven Lift-dimension Linear Power Flow

Li Guo, *Member*, *IEEE*, *Member*, *CSEE*, Zhaoning Liu, Zhongguan Wang, *Member*, *IEEE*, Xialin Li, *Member*, *IEEE*, *Member*, *CSEE*, Yixin Liu, Yuxuan Zhang, Xiaodi Zang, and Chengshan Wang, *Senior Member*, *IEEE*, *Fellow*, *CSEE*

***Abstract*—This paper proposes a reactive power and voltage optimal control method for wind farms based on data-driven power flow. Because no prior knowledge of wind farm parameters is necessary, the proposed method is model-free. Based on Koopman operator-based method, this paper constructs a power flow model of wind farms connected to the grid by using state space mapping and lift-dimension linearization. Considering reactive power devices such as wind turbines and static var generator (SVG) in wind farms, a global sensitivity-based reactive power and voltage linear optimization control model is proposed. Taking minimum reactive power adjustment of wind turbines and SVG as the objective function, combined with the sensitivity relationship between node voltage and reactive power injection, the proposed model-free voltage control method can realize optimal reactive power distribution, effectively reduce active power loss, and satisfy the requirement of rapid voltage control response of wind farms. Based on historical data of a wind farm in Ningxia, feasibility of the proposed voltage optimal control method under inaccurate parameters is verified. Compared with model-based methods, the proposed method exhibits advantages on parameter dependency and efficiency.**

***Index Terms*—Date-driven, power flow, reactive power, sensitivity, voltage control, wind power generation.**

I. INTRODUCTION

THE large-scale integration of wind power generation exerts an increasing influence on operation of power systems. Due to its inherent fluctuation, intermittence and uncertainty, high-penetration wind power generation poses challenges to voltage stability in the operation process, and affects power supply reliability and power quality of power systems [1]. To address this problem, many countries have enhanced standards and grid codes to require wind turbines have the ability to provide reactive power support in response to voltage fluctuation. On the other hand, with increase of wind farm capacity, voltage of point of common coupling (PCC) and wind turbine terminal suffers from the risk of exceeding the limit, which can result in wind turbines dropping off and causing serious imbalance between power supply and consumption [2]. Therefore, it is of great significance to pay attention to reactive power and voltage optimal control of wind farms.

In fact, extensive research on voltage control of wind farms has been carried out. Conventionally, wind farm voltage control mainly relies on the regulation capacity of reactive power devices installed to secondary-side bus. Using fast response and steady-state voltage control characteristics of static VAR compensator (SVC), SVG and static synchronous compensator (STATCOM), wind farms can provide VAR support to power grids. For instance, [3] proposes a control strategy of STATCOM to suppress voltage fluctuation of a weak loop power system. Comparing the reactive compensation capability between SVC and STATCOM, [4] proposes a fast coordinated reactive power and voltage control strategy for doubly fed induction generators (DFIGs) and STATCOM. In [5], the proposed method comprehensively coordinates reactive power compensation devices such as STATCOM, SVG and on load tap changer (OLTC) in wind farms to maintain bus voltage within feasible range. In order to solve the voltage unbalance problem induced by wind power integration, an improved voltage control strategy with strong dispatching ability for grid voltage and reactive current is proposed in [6].

Compared to reactive power devices, by using vector control technique to control active power and reactive power separately [7], wind turbines inherently possess reactive power regulation capability, and have the advantage of saving investment cost. Therefore, instead of running in constant power factor mode, operators gradually require wind turbines to provide reactive power support. Based on this idea, [8] constructs a detailed model of DFIG, and analyzes different combinations of reactive power control of rotor-side converter and grid-side converter, to achieve the purpose of optimal voltage control. In [9], a flexible compensation strategy for DFIG connected to unbalanced weak networks is proposed, which can solve the problem of voltage fluctuation at the PCC and balance output current of DFIGs. Despite focusing on the coordination of wind turbines and reactive power devices, these papers haven't taken voltage profile in wind farms into consideration. The

Manuscript received January 20, 2022; revised May 26, 2022; accepted June 23, 2022. Date of online publication June 27, 2023; date of current version August 31, 2023. This work was supported by the State Key Laboratory of Power System and Generation Equipment (SKLD21KM03) and National Natural Science Foundation of China (52007129).

L. Guo, Z. N. Liu, Z. G. Wang (corresponding author, email: wang_zg@tju.edu.cn), X. L. Li, Y. X. Liu, Y. X. Zhang, X. D. Zang, and C. S. Wang are with the School of Electrical and Information Engineering, Tianjin University, Tianjin 300072, China.

DOI: 10.17775/CSEEJPES.2022.00500

consequent drawbacks can result in large power losses and overvoltage problems at wind turbine terminals.

Using an internal network model of wind farms, [10] proposes a strategy to coordinate active power and reactive power control of DFIGs to realize optimal voltage control. In [11], the authors propose a voltage feedback control method based on decentralized gradient descent to optimally coordinate the voltage set point of wind turbines. A distributed online voltage control algorithm based on dual decomposition to coordinate reactive power output of wind turbines and reactive power devices to maintain internal bus voltage of wind farms within feasible range is proposed in [12]. A distributed cooperative secondary unbalanced voltage control strategy is proposed to decrease the output voltage unbalance factor of each droop-controlled distributed generation in [13]. In [14], an attack-resilient optimal voltage control method is proposed to eliminate the influence of cyber-attacks on voltage optimized control. Although they can coordinate all reactive power devices to optimize the internal voltage profile of wind farms, these methods rely heavily on accuracy of model parameters and cannot meet requirement of rapid voltage control response. Usually in a wind farm, feeder parameters are estimated according to length and type, and hence a complete model with accurate parameters is difficult to guarantee. The deviation of model parameters will inevitably affect the optimization results of reactive power and voltage.

Sensitivity-based voltage regulation has the advantage of fast local response. For instance, [15] takes PCC of wind farms as the control object and initial steady-state voltage as the control target, and dynamically adjusts reactive power of the wind farm according to traditional sensitivity to maintain voltage stability. On the basis of sensitivity matrix, an analytical target cascading based distributed optimal voltage control scheme for a large-scale wind farm cluster is proposed in [16]. Although having unique advantages in fast response, the traditional sensitivity method for voltage control can only achieve approximate linear near the operating point, rather than global optimal reactive power distribution. If the reactive power adjustment is large, accuracy cannot be guaranteed. Furthermore, the sensitivity calculation still relies on model parameters of the wind farm, and consequently causes the method to be invalid under the condition of incomplete model.

In order to overcome difficulties of voltage control under inaccurate model parameters, our previous work [17] utilizes a data-driven method to construct a linear power flow model based on state space mapping. However, it is difficult to solve optimization problems by using this linearized power flow, because there exists a nonlinear relationship between original input variables and augmented input variables. In addition, [18] provides pioneer work on data-driven power flow, which has satisfactory calculation speed and accuracy. The proposed data-driven method serves as the basis for accurate linearization and optimization model. A data-driven power flow linearization method under measurement noise is proposed in [19], which has higher computational accuracy than model-based methods. These works can prove that compared with traditional methods based on physical mechanism, data-driven methods can construct a power flow model under inaccurate parameters. In [20], a data-driven model-free VVC method is presented in this paper which only relies on partial measurements of critical nodes in ADNs, and the power flow performance for calculating active and reactive power is improved, but it can only ensure voltage balance and cannot achieve reactive power optimization. The authors of [21] compare sensitivity derived from model parameters with sensitivity calculated by using data-driven method, and prove the data-driven approach has good accuracy. However, it cannot apply the advantage to optimal control problems. In [22], reactive power and voltage characteristics of wind farms are determined by using historical data. The paper realizes modeling based on curve fitting, which provides a novel idea for voltage control. However, the proposed method is confined to analyzing the relationship between reactive power and voltage, and fails to coordinate wind turbines and other reactive power devices based on the data-driven model. A method based on traditional voltage sensitivity to control reactive power for voltage regulation of wind power systems is proposed in [23], and [24] uses an optimal power flow method to construct power flow equations. The two methods can be used for reactive power and voltage optimization control, but rely heavily on accuracy of model parameters.

This paper presents a data-driven optimal reactive power and voltage optimization method for wind farms based on data-driven power flow. By using Koopman lift-dimension linearization-based mapping, original state space of power flow is augmented to a high-dimensional space, by which accurate global sensitivity independent of model parameters is derived, and the reactive power and voltage linear optimization model of the wind farm is constructed. In the control process, though sensitivity is used to construct an optimization model, network topology and parameters are not prerequisite knowledge for voltage control, and the model is only an intermediate produce. Therefore, the proposed method is model-free and can resist parameter errors. To the best of the authors' knowledge, this paper makes the following contributions:

This paper presents a model-free optimal reactive power and voltage optimization method for wind farms based on data-driven power flow. By using Koopman lift-dimension linearization-based state space mapping, accurate global sensitivity independent of model parameters is derived, and the reactive power and voltage linear optimization model of the wind farm is constructed. To the best of the authors' knowledge, this paper makes the following contributions:

1) A model-free global linearization sensitivity calculation method is proposed. Based on the data-driven linearized power flow equation, voltage sensitivity is derived. Compared with traditional equilibrium point linearization method based on Jacobian matrix; it applies to a wider control range.

2) An optimal voltage control model of wind farm based on data-driven sensitivity is constructed. Having the advantage of fast solving, the linear optimization model considers the internal voltage profile in the wind farm, and avoids overvoltage problems of wind turbines. Besides, the wind farm can respond to voltage fluctuation of system-side automatically, and reduce active power losses and operation cost.

The remainder of the paper is organized as follows. Section II describes the voltage optimization model based on classical linear power flow model. The Koopman-based model-free state space mapping and sensitivity calculation method is proposed in Section III. Taking an actual wind farm in Ningxia as example, feasibility of the reactive power and voltage optimization control method is verified in Section IV. Finally, Section V concludes the paper.

II. Optimal Voltage Control Model of Wind Farm

A. Wind Farm Linear Power Flow and Voltage Model

Since topology of wind farms are usually radial networks, the wind farm voltage model takes a radial network as research object. Wind turbines are integrated to different nodes of the network, and active power injection may cause terminal voltage of feeders to be higher than the substation of the wind farm.

In order to simplify expression, it is defined that $N = \{0, 1, \cdots, N\}$ represents the set composed of nodes in the wind farm, and $L = \{l_{ij}\} \subset N \times N$ represents the set composed of branches connecting node i and node j. Node 0 represents voltage reference node. Generally, it represents high-voltage bus of the substation. Voltage magnitude of node i is represented by V_i, and p_i, q_i respectively represent active power and reactive power of node i. Branch resistance and reactance value of branch l_{ij} are respectively, represented by r_{ij} and x_{ij}, and P_{ij} and Q_{ij} represent active power and reactive power flow from the head-end of node i to node j. For convenience, downstream adjacent nodes of node i are defined as nodes farther from the reference node than node i, and directly connected to node i. The set composed of downstream adjacent nodes of node i are defined as $N_i \subset N$.

According to the above definition, we can get the following branch-form power flow equations [18]:

$$P_{ij} - \sum_{k \in N_j} P_{jk} = -p_j + r_{ij} \frac{P_{ij}^2 + Q_{ij}^2}{V_i^2} \tag{1}$$

$$Q_{ij} - \sum_{k \in N_j} Q_{jk} = -q_j + x_{ij} \frac{P_{ij}^2 + Q_{ij}^2}{V_i^2} \tag{2}$$

$$V_i^2 - V_j^2 = 2(r_{ij} P_{ij} + x_{ij} Q_{ij}) - (r_{ij}^2 + x_{ij}^2) \frac{P_{ij}^2 + Q_{ij}^2}{V_i^2} \tag{3}$$

Under voltage control, voltage of each node of the wind farm in normal conditions is usually close to nominal value, i.e., $V_i \approx 1$. Besides, losses account for a relatively small proportion of power consumption. In order to further derive the linearized branch-form power flow equation, the quadratic term on the right side of (1)–(3), which correspond to active and reactive losses in the branch, can be left out. In this way, the linearized approximate results of the original branch power flow model can be obtained:

$$P_{ij} - \sum_{k \in N_j} P_{jk} = -p_j \tag{4}$$

$$Q_{ij} - \sum_{k \in N_j} Q_{jk} = -q_j \tag{5}$$

$$V_i - V_j = r_{ij} P_{ij} + x_{ij} Q_{ij} \tag{6}$$

To simplify the expression in matrix form, $\boldsymbol{M}^0$ is defined to represent the node-branch incidence matrix of the internal network of the wind farm, of which size is $N \times (N-1)$. If node $j \in N_i$, we have elements $M_{il}^0 = 1$ and $M_{jl}^0 = -1$, where l is number of branch l_{ij}. Removing the first row corresponding to reference node 0 in matrix $\boldsymbol{M}^0$, we use $\boldsymbol{M}$ to represent the $N \times N$ dimensional node-branch incidence matrix of the remaining part, which is a full-rank square matrix. In this way, the matrix-form branch active and reactive power equations can be expressed as:

$$\boldsymbol{MP} = \boldsymbol{p} \tag{7}$$

$$\boldsymbol{MQ} = \boldsymbol{q} \tag{8}$$

where $\boldsymbol{P}$ and $\boldsymbol{Q}$ represent column vectors composed of branch active power P_{ij} and reactive power Q_{ij}, respectively, and $\boldsymbol{p}$ and $\boldsymbol{q}$ represent column vectors composed of active power injection p_i and reactive power injection q_i, respectively. Besides, the matrix form of branch voltage (6) can be expressed as:

$$(\boldsymbol{M}^0)^{\mathrm{T}} [V_0 \boldsymbol{V}^{\mathrm{T}}]^{\mathrm{T}} = \boldsymbol{m}_0 V_0 + \boldsymbol{M}^{\mathrm{T}} \boldsymbol{V} = \boldsymbol{D}_r \boldsymbol{P} + \boldsymbol{D}_x \boldsymbol{Q} \tag{9}$$

where $\boldsymbol{V}$ represents column vector composed of node voltage magnitude V_i, $\boldsymbol{m}_0^{\mathrm{T}}$ represents first row in matrix $\boldsymbol{M}^0$, and $\boldsymbol{D}_r$ and $\boldsymbol{D}_x$ represent $N \times N$ diagonal matrix with diagonal entries r_{ij} and x_{ij}, respectively.

Substituting (7) and (8) into (9), yields

$$\begin{aligned} \boldsymbol{V} &= \boldsymbol{M}^{-\mathrm{T}} (\boldsymbol{D}_r \boldsymbol{P} + \boldsymbol{D}_x \boldsymbol{Q} - \boldsymbol{m}_0 V_0) \\ &= \boldsymbol{M}^{-\mathrm{T}} \boldsymbol{D}_r \boldsymbol{P} + \boldsymbol{M}^{-\mathrm{T}} \boldsymbol{D}_x \boldsymbol{Q} - \boldsymbol{M}^{-\mathrm{T}} \boldsymbol{m}_0 V_0 \\ &= \boldsymbol{M}^{-\mathrm{T}} \boldsymbol{D}_r \boldsymbol{M}^{-1} \boldsymbol{p} + \boldsymbol{M}^{-\mathrm{T}} \boldsymbol{D}_x \boldsymbol{M}^{-1} \boldsymbol{q} - \boldsymbol{M}^{-\mathrm{T}} \boldsymbol{m}_0 V_0 \end{aligned} \tag{10}$$

By making the following definition:

$$\boldsymbol{R} = \boldsymbol{M}^{-\mathrm{T}} \boldsymbol{D}_r \boldsymbol{M}^{-1} \tag{11}$$

$$\boldsymbol{X} = \boldsymbol{M}^{-\mathrm{T}} \boldsymbol{D}_x \boldsymbol{M}^{-1} \tag{12}$$

the voltage (10) can be rewritten as:

$$\begin{aligned} \boldsymbol{V} &= \boldsymbol{Rp} + \boldsymbol{X}(\bar{\boldsymbol{q}} + \Delta \boldsymbol{q}) - \boldsymbol{M}^{-\mathrm{T}} \boldsymbol{m}_0 V_0 \\ &= \boldsymbol{X} \Delta \boldsymbol{q} + \bar{\boldsymbol{V}} \end{aligned} \tag{13}$$

where $\bar{\boldsymbol{q}}$ represents the vector composed of reactive power injection without voltage control, $\Delta \boldsymbol{q}$ represents the vector composed of reactive power adjustment, and $\bar{\boldsymbol{V}}$ represents the natural voltage profile of the wind farm without reactive power adjustment. Specifically, it corresponds to

$$\bar{\boldsymbol{V}} = \boldsymbol{Rp} + \boldsymbol{X} \bar{\boldsymbol{q}} - \boldsymbol{M}^{-\mathrm{T}} \boldsymbol{m}_0 V_0 \tag{14}$$

In the voltage optimal control model, $\bar{\boldsymbol{V}}$ can be considered a constant. The linear sensitivity relation between node voltage and wind turbines reactive power is described in (13). It should be noted expression is based on the assumption of flat voltage profile $V_i \approx 1$, and leaves out loss term, which definitely deteriorates the linear model accuracy. From another perspective, if $\boldsymbol{X}$ is derived by using the sensitivity analysis method based on Jacobian matrix in Newton-Raphson method, satisfactory linearized approximation only can be obtained in a small range near the equilibrium point. In addition, whether using linear power flow in (13) or equilibrium point sensitivity based on Jacobian matrix, the relation between voltage and reactive power is still derived based on model parameters. In conditions of inaccurate parameters, voltage control performance will be consequentially limited. Therefore, a model-free state space mapping-based linear power flow and voltage control method is proposed in Section III to avoid dependency on model parameters.

B. Voltage Optimization Model of Wind Farm

Based on the linear relation between voltage and reactive power (13), a wind farm voltage optimization control model can be constructed. Reactive power regulation capacity of wind turbines should be considered in the model. In response to voltage fluctuation of the PCC, according to predetermined characteristics of automatic voltage control (AVC), the wind farm is required to regulate reactive power to meet the droop relationship between reactive power via the PCC and high-voltage bus voltage of the substation. In the meantime, wind farm voltage control needs to ensure internal voltage balance, without voltage violation at wind turbine terminals, and reactive power distribution among wind turbines should be improved considering minimum adjustment amount. Based on the above objectives and constraints, a voltage optimization model can be constructed.

1) Optimization Objective

With AVC and internal voltage constraints, the objective is to minimize reactive power adjustment of wind turbines and SVG to prolong their lifetimes. Therefore, the optimization objective can be expressed as:

$$\Delta \boldsymbol{q}^{*}=\arg\min\|\Delta \boldsymbol{q}\|_2^2=\arg\min\sum_{i=1}^{N}\Delta q_i^2 \tag{15}$$

where $\Delta \boldsymbol{q}^*$ represents optimal reactive power adjustment vector, $\|\cdot\|_2^2$ represents Euclidean norm, and Δq_i represents reactive power adjustment of the wind turbine at node i.

2) Constraints

Constraints of wind farm voltage optimization include wind farm reactive power output constraints, voltage and reactive power flow constraints, voltage magnitude constraints, wind turbines and SVG capacity constraints, reactive power ramping rate constraints, and power factor constraints. Voltage and reactive power flow constraints can be represented by (13), and complete constraints can be expressed as

$$-q_0=q_{\mathrm{ref}}-K_f(V_0-V_{\mathrm{ref}}) \tag{16a}$$

$$\boldsymbol{V}_{\min}\leq\bar{\boldsymbol{V}}+\boldsymbol{X}\Delta\boldsymbol{q}\leq\boldsymbol{V}_{\max} \tag{16b}$$

$$-\boldsymbol{q}_{\max}\leq\bar{\boldsymbol{q}}+\Delta\boldsymbol{q}\leq\boldsymbol{q}_{\max} \tag{16c}$$

$$-\Delta\boldsymbol{q}_{\max}\leq\Delta\boldsymbol{q}\leq\Delta\boldsymbol{q}_{\max} \tag{16d}$$

$$\sqrt{p_i^2+(\bar{q}_i+\Delta q_i)^2}\leq S_{i,\max},\ \text{for all } i\in N \tag{16e}$$

$$\cos\varphi_i=\frac{p_i}{\sqrt{p_i^2+(\bar{q}_i+\Delta q_i)^2}}\geq 0.7,\ \text{for all } i\in N \tag{16f}$$

$$\sum_{i=0}^{N}p_i=0 \tag{16g}$$

$$\sum_{i=0}^{N}(\bar{q}_i+\Delta q_i)=0 \tag{16h}$$

where q_{ref} represents set point of wind farm reactive power output, V_{ref} represents set point of wind farm PCC voltage, K_f represents droop coefficient between wind farm reactive power output and PCC voltage, $\boldsymbol{V}_{\min}$, $\boldsymbol{V}_{\max}$ represent vectors composed of voltage magnitude bounds, $\boldsymbol{q}_{\max}$ represents vectors composed of maximum reactive power limits, $\Delta\boldsymbol{q}_{\max}$ represents vectors composed of maximum reactive power ramping rate limits, $\bar{q}_i$ represents reactive power injection of node i without voltage control, $S_{i,\max}$ represents capacity limit of node i, and $\cos\varphi_i$ represents power factor of node i.

In the voltage optimization model (15) and (16), if the voltage and reactive power sensitivity matrix $\boldsymbol{X}$ have been obtained, the optimization model is simplified as a linear constrained quadratic programming problem, which can be solved in a very short time. However, due to the reason explained above, value of $\boldsymbol{X}$ derived from the linear power flow equation suffers from large approximation errors, which may impose an adverse influence on voltage control performance. On the other hand, the local linearization method based on Jacobian matrix only exhibits acceptable linear characteristics near the operation point, both methods rely heavily on accuracy of model parameters. Without accurate model parameters, voltage control effect based on linear optimization model (15) and (16) is difficult to be guaranteed. Therefore, it is necessary to propose a model-free voltage control method independent of parameters to realize optimal reactive power distribution, which can utilize real operation data to obtain high-precision global sensitivity matrix $\boldsymbol{X}$.

III. Lift-Dimension Mapping-Based Power Flow and Sensitivity Calculation

A. Data-Driven Voltage Optimal Control Framework

In this paper, a data-driven method based on Koopman operator is used to construct a lift-dimension linear power flow, and voltage and reactive power sensitivity matrix $\boldsymbol{X}$ in the optimization model (16) is derived by using state space mapping. Compared with methods based on impedance parameters; the proposed method is independent of accuracy of model parameters because the sensitivities are derived from real operation data. The voltage control framework can be divided into two levels: offline data-driven model training level and online voltage optimization level:

1) Offline data-driven model training level: Collect historical reactive power injection and voltage magnitude as training sample input, construct lift-dimension linear power flow model based on Koopman state space mapping, and calculate global sensitivity matrix $\boldsymbol{X}$ in an offline manner.

2) Online voltage optimization level: According to real operation state of the wind farm, construct linear constrained quadratic programming model (15) and (16) based on sensitivity matrix $\boldsymbol{X}$ obtained from model training level. By solving

the model, reactive power adjustment is issued to each wind turbine and SVG to realize optimal voltage control.

The data-driven voltage optimal control framework is shown in Fig. 1. In order to facilitate understanding, the physical level of the wind farm, i.e., wind turbines, is also drawn in the framework. Since the online voltage optimization layer needs to collect real-time operation status of the wind farm and perform online control, the physical level illustrates data flow of the proposed method. Because data-driven model training carries out sensitivity calculation based on lift-dimension linear power flow, sensitivities are global results instead of local linearization around the equilibrium point, and values can apply to a wide range if network topology maintains unchanged. The voltage optimization model is constructed based on voltage measurement of the PCC, voltage measurement of nodes in the wind farm, power output real-time value of wind turbines and SVG. Combined with data-driven trained global sensitivities, the voltage optimization model is updated in a rolling manner to achieve online optimal voltage control. Therefore, in each optimization cycle, the control system uses the linear model obtained from data-driven model training level to reconstruct voltage optimization model based on operation status. Owing to the simple form of optimization model, though voltage control method is centralized, fast online solution can be achieved within the cycle. Utilizing double-layer model training and voltage optimization, unified offline training and online control is realized. In conclusion, though the data-driven power flow is a global model, the proposed method can cope with frequency disturbance of wind power.

B. Koopman-Based Lift-Dimension Linear Power Flow

In nature, the accurate power flow model of the wind farm is a nonlinear equation. According to the Koopman operator, a nonlinear equation can be transformed into an infinite-dimensional linear equation by using state space mapping. In practice, it is sufficient to highly fit the original nonlinearity by lifting state space to several thousand dimensions, rather than infinite dimensions. Therefore, the essence of power flow modeling based on Koopman operator is to utilize a large amount of historical operation data to train the lift-dimension linear model. Samples are used to fit the linear relationship between state variables and input variables in the lift-dimension space. Specifically, it is assumed the wind farm satisfies the following nonlinear power flow model:

$$\boldsymbol{y} = \varphi(\boldsymbol{x}) \tag{17}$$

where state variables $\boldsymbol{y} = [\boldsymbol{\theta} \quad \boldsymbol{V}]^{\mathrm{T}}$ are composed of phase angle and voltage magnitude, and K-dimensional input variables $\boldsymbol{x} = [\boldsymbol{p} \quad \boldsymbol{q}]^{\mathrm{T}}$ are composed of active power and reactive power injection.

By increasing dimension of input variables to construct a linear relationship, the coordinate system is extended, and the global linearization equation can be derived. Specifically, with lift-dimension function $\boldsymbol{\psi}(\boldsymbol{x})$, there exists a linear matrix $\boldsymbol{C}$, by which the relationship between state variables and input variables can be expressed [16]:

$$\boldsymbol{y} = \boldsymbol{C}\boldsymbol{x}_{\mathrm{lift}} = [\boldsymbol{C}_1\boldsymbol{C}_2]\begin{bmatrix}\boldsymbol{x}\\ \boldsymbol{\psi}(\boldsymbol{x})\end{bmatrix} \tag{18}$$

where $\boldsymbol{x}_{\mathrm{lift}}$ represents the vector composed of augmented input variables.

Theoretically, the linear equation can be globally strictly true only if lift-dimension function $\boldsymbol{\psi}(\boldsymbol{x})$ is infinite, but in practical application, an acceptable linear approximation can be obtained by increasing input variables to appropriate dimensions. Assume the dimension of the augmented input

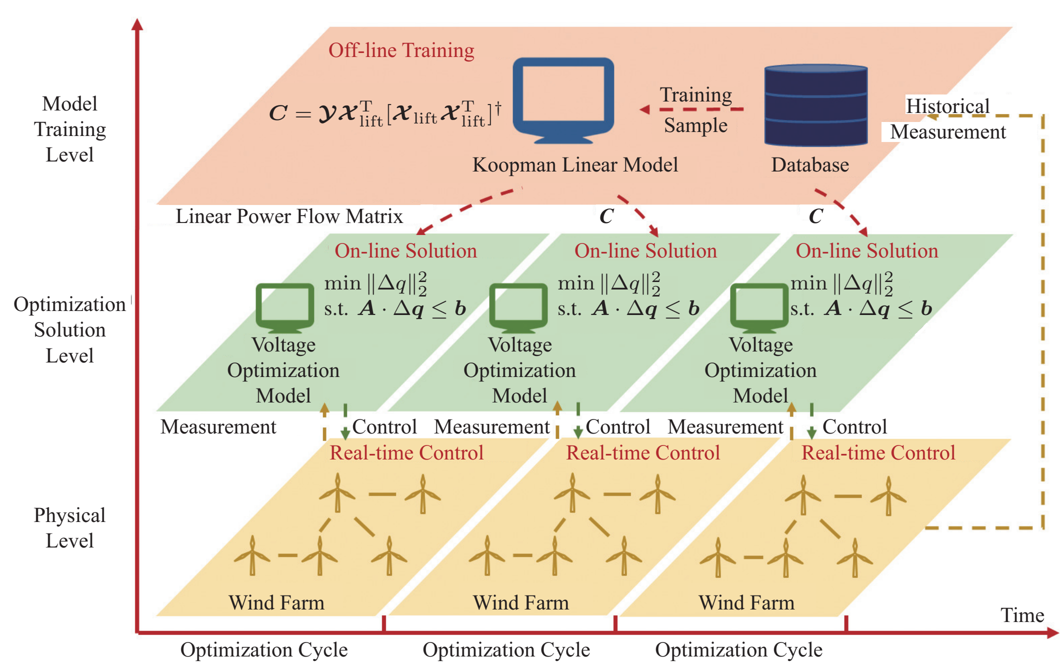

Fig. 1. Data-driven voltage optimal control framework.

variables is n, and the i-th augmented input variable, $\psi_i(\boldsymbol{x})$, can be defined as a function of $\boldsymbol{x}$:

$$\psi_i(\boldsymbol{x}) = f_{\text{lift}}(\boldsymbol{x} - \boldsymbol{c}_i) \tag{19}$$

where $\boldsymbol{c}_i$ represents the i-th K-dimensional basis vector in which elements are random within the variable range.

In the paper, the lift-dimension function f_{lift} adopts poly-harmonic form [16], i.e.,

$$f_{\text{lift}}(\boldsymbol{x} - \boldsymbol{c}_i) = \sqrt{\sum_{j=1}^{K}(x_j - c_{ij})^2} \cdot \ln \sqrt{\sum_{j=1}^{K}(x_j - c_{ij})^2} \tag{20}$$

where x_j represents the j-th element of input variables $\boldsymbol{x}$, c_{ij} represents the j-th element of $\boldsymbol{c}_i$.

In order to obtain the linear relationship (18) in the lift-dimension state space, linear power flow matrix $\boldsymbol{C}$ can be fitted by using the least squares estimation according to the massive historical samples. Assuming historical samples used for matrix training contain S time sections, the sample set of input variables $\boldsymbol{X}$, and sample set of output variables $\boldsymbol{Y}$ can be defined as:

$$\boldsymbol{X} = [\boldsymbol{x}_1 \boldsymbol{x}_2 \cdots \boldsymbol{x}_{\text{S}}] \tag{21}$$

$$\boldsymbol{Y} = [\boldsymbol{y}_1 \boldsymbol{y}_2 \cdots \boldsymbol{y}_{\text{S}}] \tag{22}$$

where $\boldsymbol{x}_i$ and $\boldsymbol{y}_i$ represent input variables and state variables of i-th time section, respectively. Therefore, we can get the sample set of augmented input variables $\boldsymbol{X}_{\text{lift}}$ according to $\boldsymbol{X}$:

$$\boldsymbol{X}_{\text{lift}} = [\boldsymbol{x}_{\text{lift},1} \boldsymbol{x}_{\text{lift},2} \cdots \boldsymbol{x}_{\text{lift},S}] \tag{23}$$

where $\boldsymbol{x}_{\text{lift},i}$ represents augmented input variables of i-th time section, which can be calculated according to

$$\boldsymbol{x}_{\text{liftt},i} = \begin{bmatrix} \boldsymbol{x}_i \\ \boldsymbol{\psi}(\boldsymbol{x}_i) \end{bmatrix} \tag{24}$$

Therefore, using the above sample sets, linear matrix $\boldsymbol{C}$ can be fitted according to least squares estimation:

$$\boldsymbol{C} = \boldsymbol{Y} \boldsymbol{X}_{\text{lift}}^{\text{T}} [\boldsymbol{X}_{\text{lift}} \boldsymbol{X}_{\text{lift}}^{\text{T}}]^{\dagger} \tag{25}$$

where $[\cdot]^{\dagger}$ represents the Moore-Penrose inverse of matrix.

Using linear power flow matrix $\boldsymbol{C}$ calculated in (25), the linear relationship between state variables $\boldsymbol{y}$ and augmented input variables $\boldsymbol{x}_{\text{lift}}$ can be described without model parameters. The lift-dimension linear power flow equation is independent of parameters, and is not based on linearization near the equilibrium point. Therefore, the global linear relationship can be obtained by state space mapping, which exhibits significant advantages in voltage optimization control.

C. Data-Driven Sensitivity Matrix Calculation

With incomplete model parameters, the high-precision global linear power flow equation can be trained based on historical data. Based on linear power flow matrix $\boldsymbol{C}$, a more accurate sensitivity matrix $\boldsymbol{X}$ can be derived and used in voltage optimization model (16), and hence voltage optimal control independent of parameters can be realized.

The element in the i-th row and j-th column of the sensitivity matrix $\boldsymbol{X}$ can be represented as X_{ij}. For convenience, we define that it represents sensitivity of voltage magnitude of node i to reactive power of node j.

In fact, linear power flow matrix $\boldsymbol{C}$ reveals the linear relationship between node voltage and reactive power. Therefore, accurate sensitivity can be derived based on the global linear power flow equation. Specifically, sensitivity X_{ij} can be calculated according to

$$X_{ij} = \frac{\partial V_i}{\partial \Delta q_j} = C_{ij} + \sum_{t=1}^{n}\left(C_{i,(K+k)} \cdot \frac{\partial \psi_k(\boldsymbol{x})}{\partial \Delta q_j}\right) \tag{26}$$

where C_{ij} represents the linear relationship between voltage magnitude of node i, V_i, and reactive power adjustment of node j, Δq_j, $C_{i,(K+k)}$ represents the linear relationship between voltage magnitude of node i, V_i, and the k-th augmented input variables $\psi_k(\boldsymbol{x})$, and the partial derivative term on the right side can be calculated according to

$$\frac{\partial \psi_k(\boldsymbol{x})}{\partial \Delta q_j} = \frac{(\Delta q_j - c_{kj}) \ln\left(e\sqrt{\sum_{t=1}^{K}(x_t - c_{kt})^2}\right)}{\sqrt{\sum_{k=1}^{K}(x_t - c_{kt})^2}} \tag{27}$$

Therefore, value of sensitivity X_{ij} between any node voltage and reactive power can be obtained based on linear power flow matrix $\boldsymbol{C}$ trained by offline data-driven training, basis vector $\boldsymbol{c}_i$, and reactive power adjustment measurement Δq_j. Using global sensitivity result $\boldsymbol{X}$, complete wind farm voltage optimization model (15) and (16) can be constructed.

In practical applications, linear power flow matrix $\boldsymbol{C}$ can be regarded as a constant parameter after offline training. It is unnecessary to update value of $\boldsymbol{C}$ frequently if wind farm topology remains unchanged. On the other hand, sensitivity matrix $\boldsymbol{X}$ can be calculated in an online manner according to (26) and (27) based on linear power flow matrix $\boldsymbol{C}$ according to operation state of the wind farm. Reactive power regulation instructions of wind turbines and SVG can be obtained by solving the online optimization model. To deal with change of operation state, sensitivity matrix $\boldsymbol{X}$ and the optimization model should be updated periodically to realize online optimal voltage control. The complete process of the proposed model-free voltage control method based on lift-dimension linear power flow is shown in Fig. 2.

Owing to simple sensitivity calculation without repetitive data-driven training, and simple linear constrained form of the optimization model, the proposed method can meet requirements of fast dynamic voltage control and response to AVC command.

IV. CASE STUDY

A. Basic Test System and Parameters

Case study simulation is carried out based on real parameters and operation data from an actual wind farm located in Ningxia Autonomous Region, China. The feeder topology of the wind farm is shown in Fig. 3.

As shown in the figure, there are 48 wind turbines in the wind farm, with a total installed capacity of 120 MW and a SVG of which the capacity is 40 MVar. The wind turbines are divided into 5 groups, which are connected to different nodes

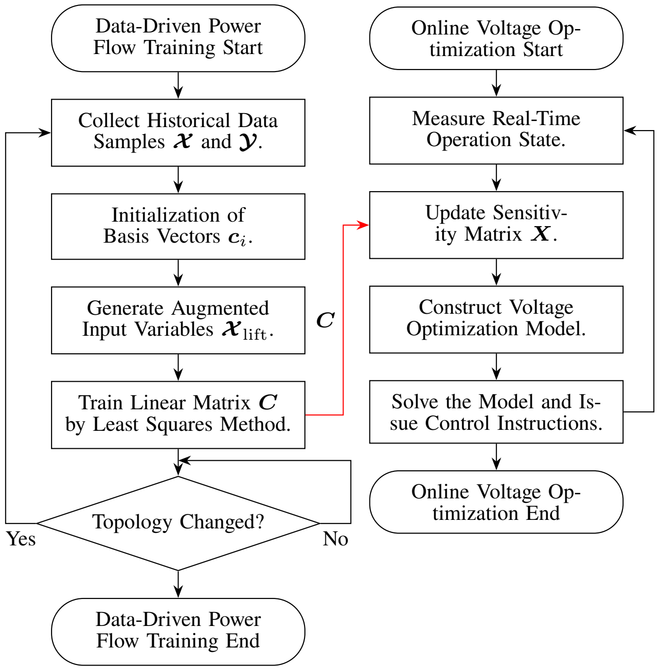

Fig. 2. Complete process of the model-free voltage control method based on lift-dimension linear power flow.

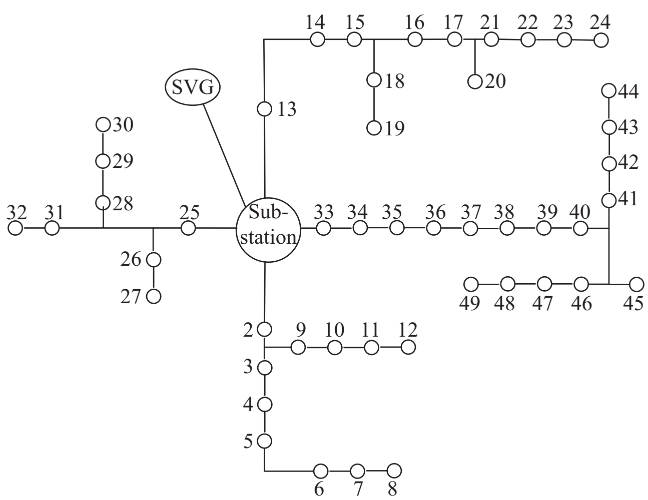

Fig. 3. Topology of the wind farm for case study.

of 35 kV feeders, and the SVG is connected to 35 kV bus in the substation, which is connected to 110 kV power grid through a 110/35 kV transformer.

B. Data-Driven Power Flow Analysis

To validate the performance of the data-driven linear power flow model, we construct the historical sample sets by using 500, 1,000, and 2,000 samples, respectively. Actual data record of active and reactive power output on 0:01 am, June 1st, 2021, is taken as initial condition. To cover more different situations, taking the initial condition as the active power and reactive power benchmark, training data are generated by scaling the initial condition with random coefficients. For each training sample, power flow calculation is executed by using MATPOWER, and the wind turbine voltage results are also taken as training samples (output samples). The training data are utilized to obtain the linear power flow matrix $\boldsymbol{C}$. Besides, we also generate 1,000 groups of test samples by scaling the initial condition with other random coefficients. The power flow results based on the proposed method (PM) model is compared with the reference method (RM) in [18], and the maximum errors and average errors of node voltage are shown in Table I. For convenience of readers to obtain the original sample data, the training data file is uploaded to Google drive [25].

As seen from Table I, the power flow results based on the proposed method possesses satisfactory high accuracy than the reference method in [18]. The advantage of our proposed method is that the augmented dimension can be adjusted to further improve the accuracy, and when the historical sample number is small, the accuracy improves with the increase of the historical sample number and lifted dimensions. It also can be concluded from the results shown in Table I that, when the number of historical sample set is sufficiently large, with the increase of the number of historical sample set and lifted dimensions, both the maximum error and the average error of power flow results tend to be stable. In other words, the proposed data-driven method can realize a satisfactory power flow analysis by using training samples without very large size. In the subsequent case analysis, the number of sample set is 2,000, and the lifted dimension is also set to be 2,000.

As a data-driven method, the proposed voltage control may be affected by data quality, and inevitable measurement errors may deteriorate the accuracy of power flow calculation. In order to further analyze the influence of data on this method, taking accurate power flow results of 2,000 groups of sample data, obtained from power flow calculation by using MATPOWER, under normal conditions as benchmark, and 500 groups, 1,000 groups and 2,000 groups of samples are randomly selected to add random disturbances within the range of $\pm$ 0.1% of real values to represent measurement errors. By

TABLE I
ERROR COMPARISON OF POWER FLOW RESULTS

Number of Historical Sample Set	Lifted Dimensions	Maximum Error (p.u.)		Average Error (p.u.)	
		PM	RM	PM	RM
500	1500	6.91×10^{-4}	2.3×10^{-3}	3.91×10^{-5}	3.9×10^{-4}
500	2000	6.81×10^{-4}	2.3×10^{-3}	3.13×10^{-5}	3.9×10^{-4}
1000	1500	6.84×10^{-4}	1.1×10^{-3}	3.74×10^{-5}	4.16×10^{-5}
1000	2000	6.31×10^{-4}	1.1×10^{-3}	2.72×10^{-5}	4.16×10^{-5}
2000	1500	6.4×10^{-4}	1.3×10^{-3}	2.94×10^{-5}	3.7×10^{-5}
2000	2000	5.27×10^{-4}	1.3×10^{-3}	2.33×10^{-5}	3.7×10^{-5}

using the proposed data-driven method, the voltage profiles under different sample sets are shown in Fig. 4.

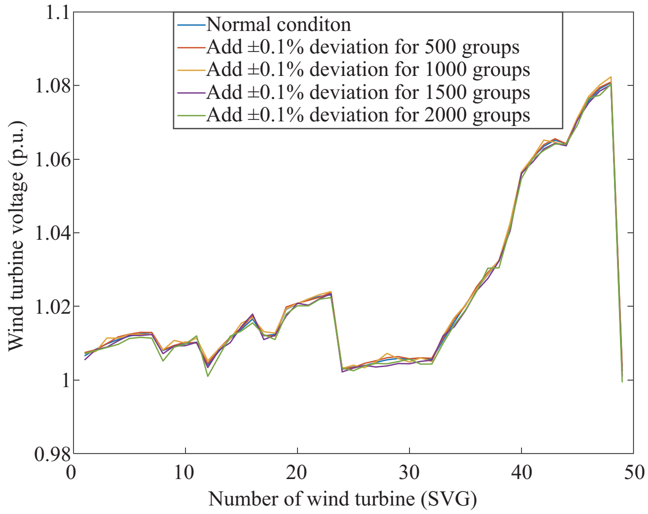

Fig. 4. Comparison of power flow accuracy under different groups of errors.

It obvious that, Fig. 4 validates that the power flow profiles under the proposed method with measurement errors are very close to the result with accurate training data. In other words, although sample size and data quality have an effect on the performance of the proposed method, a satisfactory power flow result can be guaranteed under normal sample sizes and errors. In fact, measurement errors are usually in normal distribution around real values, if measurement equipment is qualified. Therefore, the adverse effect of data accuracy can be limited to minimum extent, if only the sample size is sufficiently large.

On the other hand, the proposed data-driven power flow training is independent of model parameters, and therefore it can withstand the negative impact of parameter errors. In this way, power flow calculation accuracy can be improved and applied to different scenarios. In order to verify influence of parameter errors on the data-driven model and traditional physical model-based method, we add 15% error and 20% error to feeder parameters. At the same time, the method proposed in this paper is compared with the reference method in [18], and result comparison is shown in Fig. 5.

It can be concluded from Fig. 5 that, with inaccurate parameters, the power flow results based on Newton-Raphson method suffer from serious deviation, and the deviation further increases with greater parameter errors. In contrast, the proposed data-driven lift-dimension power flow exhibits very close results to the results based on fully accurate model. Since the value range of the training data may not cover the actual scenario of the wind farm, the linear power flow in [18] suffers from limitations, and results in errors in the voltage profile results. Compared with the results shown in Fig. 4, we can easily draw a conclusion that the influence of data accuracy under the proposed method is much smaller than parameter accuracy under model-based method. The comparison verifies the superiority of the proposed data-driven method over traditional methods, which ensures the applicability and robustness under different conditions.

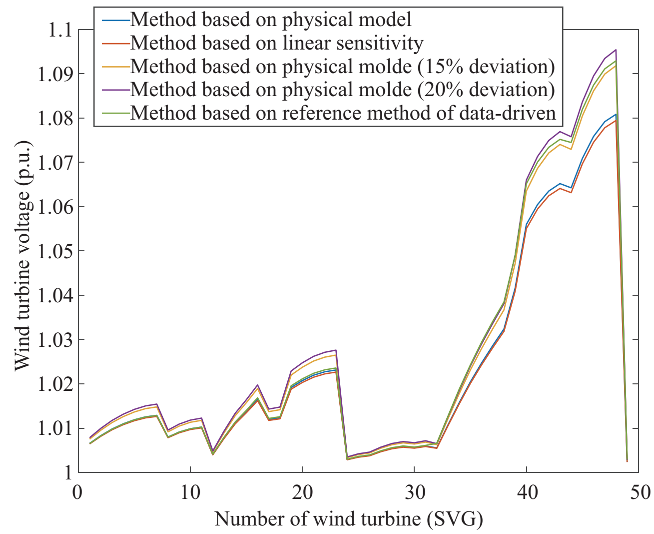

Fig. 5. Comparison of power flow accuracy under different methods.

C. *Voltage Control Analysis Under Accurate Parameters*

1) *Voltage control under normal conditions*

In this scenario, voltage control performance under normal fluctuation is discussed. Voltage of the primary-side bus in the substation is assumed to be 113.3 kV (1.03 in p.u. value), the droop coefficient is set to be 125 MVar, and total reactive power output of the wind farm via the substation is calculated according to the droop characteristics between the wind farm reactive power output and the primary-side bus voltage. Therefore, a voltage optimization model is constructed considering wind farm external characteristics requirement.

The voltage profile in the wind farm is shown in Fig. 6, and reactive power adjustment of wind turbines and SVG is shown in Fig. 7, where positive adjustment value represents increasing reactive power consumption. For comparison, results under optimal power flow method based on a fully accurate model are also shown in Fig. 6. In response to voltage fluctuation of the primary-side bus of substation, the proposed model-free method can meet the AVC requirement with more

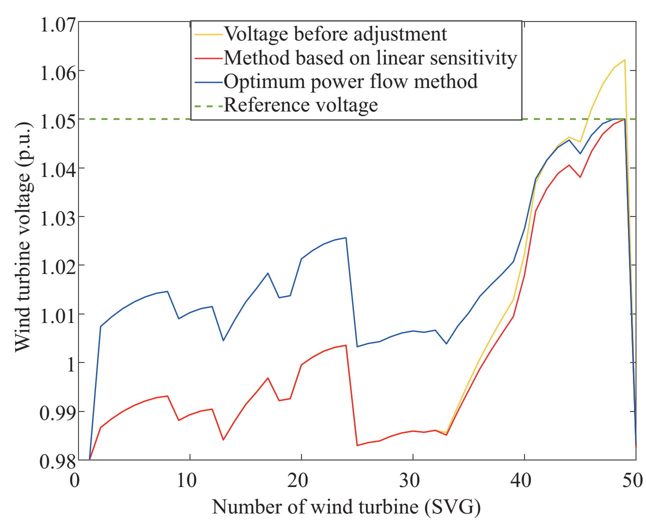

Fig. 6. Voltage control performance under normal conditions.

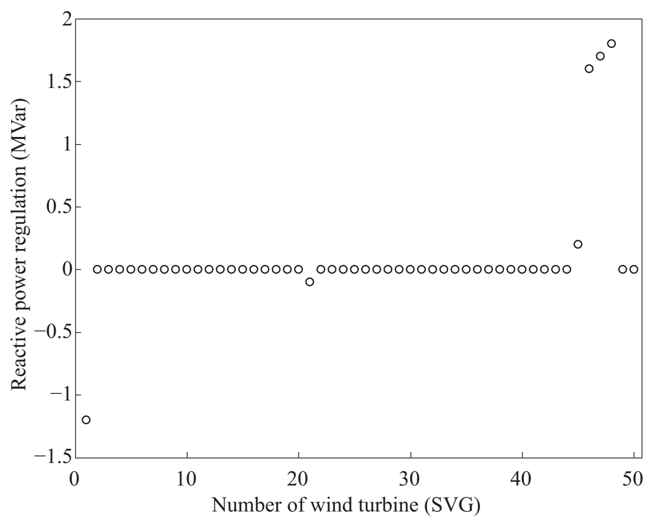

Fig. 7. Reactive power adjustment of wind turbines and SVG under normal conditions.

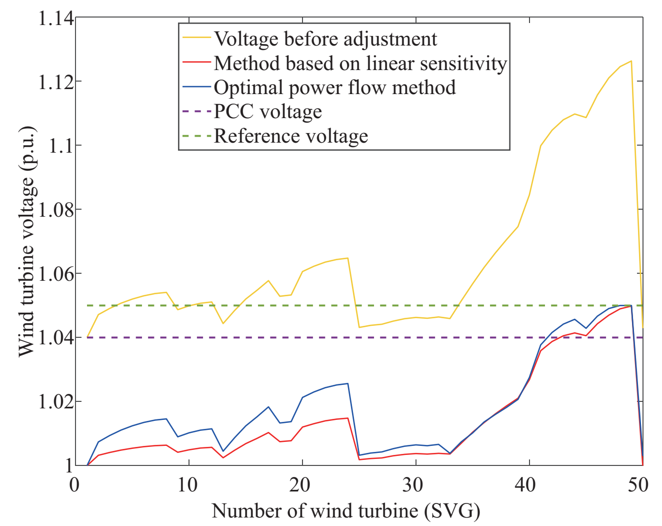

Fig. 8. Voltage control performance under extreme conditions.

reasonable voltage profile inside the wind farm. Besides, node voltage in the wind farm is maintained within the security range, which avoids overvoltage at the end of feeders before adjustment. Compared with optimal power flow method with accurate model, the average node voltage is smaller, which demonstrates performance of the proposed method.

According to reactive power adjustment amount of wind turbines in the wind farm, we execute power flow calculation based on accurate model to analyze active power loss. Table II shows relevant results of active power loss in the wind farm. As seen from Table II, by utilizing the proposed model-free voltage control method, serious voltage deviation is significantly mitigated, and hence active power loss can be reduced, which consequently saves operation cost of the wind farm.

TABLE II
MAXIMUM VOLTAGE AND ACTIVE POWER LOSS IN THE WIND FARM

Variables	1st Test	2nd Test	3rd Test
Maximum Voltage Before Voltage Control	1.067	1.069	1.064
Maximum Voltage After Voltage Control	1.048	1.049	1.048
Active Power Loss Before Voltage Control	2.34%	2.53%	2.67%
Active Power Loss After Voltage Control	1.85%	2.02%	2.12%
Reduced Active Power Loss	0.59%	0.51%	0.55%

2) Voltage Control Under Extreme Conditions

In this scenario, voltage control performance under extreme fluctuation is discussed. Voltage of the primary-side bus in the substation is assumed to be 1.04 in p.u. value, and droop coefficient is 125 MVar. Due to high PCC voltage, average voltage of the wind farm will increase. Moreover, assuming active power output of the wind farm is close to maximum capacity, voltage magnitude at the end of each feeder may exceed upper limit seriously. The voltage profile in the wind farm under the proposed method is shown in Fig. 8. For comparison, the voltage profile under optimal power flow with accurate model is also shown in Fig. 8. As seen from results, under extreme operating conditions, node voltage inside the wind farm violates upper bound severely, whereas the proposed method can still maintain wind turbine terminal voltage within the security range 0.95∼1.05. Compared with optimal power flow method with accurate model, the voltage profile is more balanced.

Reactive power adjustment of wind turbines and SVG is shown in Fig. 9, where positive adjustment value represents increasing reactive power consumption. It can be concluded reactive power adjustment of each wind turbine meets constraints of wind turbine capacity. With adequate external output characteristics of the wind farm according to AVC command, the proposed method eliminates overvoltage problem and minimum reactive power adjustment is realized.

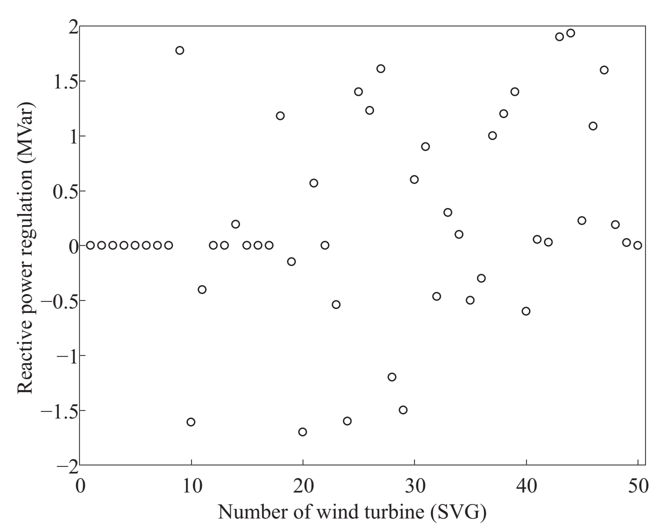

Fig. 9. Reactive power adjustment of wind turbines and SVG under extreme conditions.

D. Voltage Control Analysis Under Inaccurate Parameters

This case focuses on voltage control performance under inaccurate parameters. The proposed model-free voltage control method is compared with traditional sensitivity-based voltage control method using inaccurate parameters, and optimal power flow-based voltage control method using inaccurate parameters. A simulation test is carried out with 15% deviation added to real feeder impedance parameters of the wind farm. Voltage control results are shown in Fig. 10, and reactive power adjustment under the 3 methods is shown in Fig. 11.

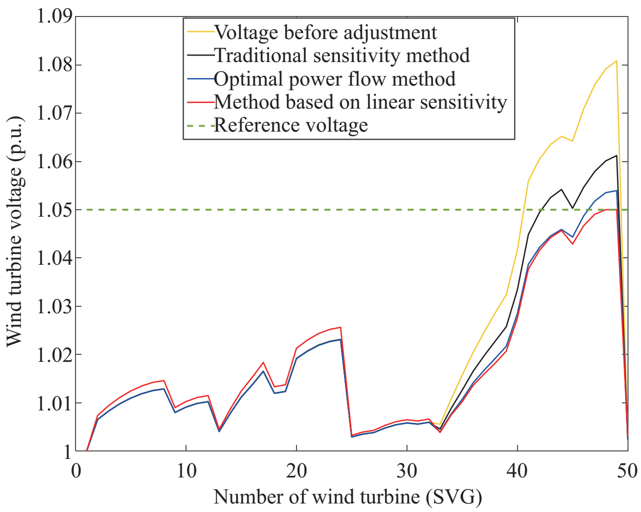

Fig. 10. Voltage control performance under inaccurate parameters.

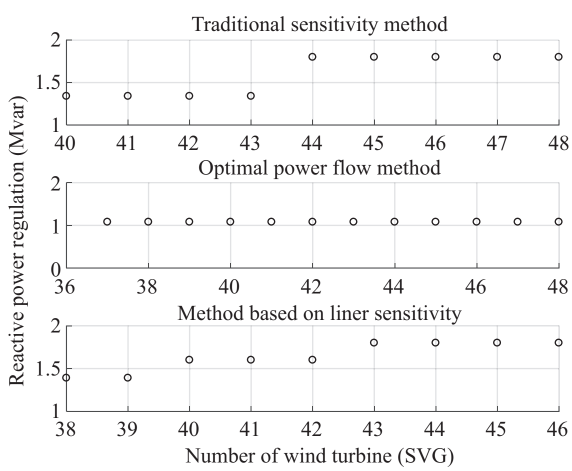

Fig. 11. Reactive power adjustment of wind turbines and SVG under inaccurate parameters.

Compared with traditional sensitivity-based voltage control method, the proposed model-free global linear voltage control method is unaffected by inaccurate parameters. With increase of parameter errors, superiority of the proposed method over traditional model-based sensitivity method is more prominent. Compared with the optimal power flow-based voltage control method, the proposed model-free global linear voltage control method applies to a wider range, and the voltage optimization model possesses simpler form, which makes the proposed method have higher solution efficiency adaptive to online applications. In conclusion, the proposed method exhibits advantages on parameter dependency and calculation efficiency over model-based methods.

V. Conclusion

Increasing penetration of wind power generation necessitates reactive power and voltage autonomous control of wind farms. In addition to meeting the external requirement of AVC, a wind farm should improve inside voltage profile and avoid overvoltage by regulating reactive power of wind turbines. This paper presents a model-free reactive power and voltage optimal control method of wind farms based on data-driven linear power flow. By utilizing Koopman operator-based method, a linear power flow model of wind farm is constructed by using state space mapping and lift-dimension linearization. Considering reactive power devices such as wind turbines and SVG, global sensitivity is derived based on data-driven power flow. Sensitivity is a global result instead of local linearization around the equilibrium point, and the value can apply to a wide range if network topology remains unchanged. Besides, the reactive power and voltage linear online optimization model is established. Taking minimum reactive power adjustment of wind turbines and SVG as objective functions, the proposed model-free voltage control method can realize optimal reactive power distribution, effectively reduce active power loss, and satisfy the requirement of rapid voltage control response of wind farms. Simulation results validate the proposed method has significant advantages on parameter dependency and calculation efficiency over model-based methods.

References

[1] L. Xie, P. M. S. Carvalho, L. A. F. M. Ferreira, J. H. Liu, B. H. Krogh, N. Popli, and M. D. Ilić, "Wind integration in power systems: operational challenges and possible solutions," *Proceedings of the IEEE*, vol. 99, no. 1, pp. 214–232, Jan. 2011.

[2] J. Lin, Y. Z. Sun, Y. H. Song, W. Z. Gao, and P. Sorensen, "Wind power fluctuation smoothing controller based on risk assessment of grid frequency deviation in an isolated system," *IEEE Transactions on Sustainable Energy*, vol. 4, no. 2, pp. 379–392, Apr. 2013.

[3] C. Han, A. Q. Huang, M. E. Baran, S. Bhattacharya, W. Litzenberger, L. Anderson, A. L. Johnson, and A. A. Edris, "STATCOM impact study on the integration of a large wind farm into a weak loop power system," *IEEE Transactions on Energy Conversion*, vol. 23, no. 1, pp. 226–233, Mar. 2008.

[4] J. Qi, W. B. Zhao, and X. Y. Bian, "Comparative study of SVC and STATCOM reactive power compensation for prosumer microgrids with DFIG-based wind farm integration," *IEEE Access*, vol. 8, pp. 209878–209885, Oct. 2020.

[5] H. R. Zhao, Q. W. Wu, Q. L. Guo, H. B. Sun, S. J. Huang, and Y. S. Xue, "Coordinated voltage control of a wind farm based on model predictive control," *IEEE Transactions on Sustainable Energy*, vol. 7, no. 4, pp. 1440–1451, Oct. 2016.

[6] S. Asadollah, R. W. Zhu, and M. Liserre, "Analysis of voltage control strategies for wind farms," *IEEE Transactions on Sustainable Energy*, vol. 11, no. 2, pp. 1002–1012, Apr. 2020.

[7] S. H. Li, T. A. Haskew, R. P. Swatloski, and W. Gathings, "Optimal and direct-current vector control of direct-driven PMSG wind turbines," *IEEE Transactions on Power Electronics*, vol. 27, no. 5, pp. 2325–2337, May 2012.

[8] M. Kayikci and J. V. Milanovic, "Reactive power control strategies for DFIG-based plants," *IEEE Transactions on Energy Conversion*, vol. 22, no. 2, pp. 389–396, Jun. 2007.

[9] T. Wang, H. Nian, Z. Q. Zhu, H. Y. Huang, and X. M. Huang, "Flexible PCC voltage unbalance compensation strategy for autonomous operation of parallel DFIGs," *IEEE Transactions on Industry Applications*, vol. 53, no. 5, pp. 4807–4820, Sep./Oct. 2017.

[10] J. X. Ouyang, T. Tang, J. Yao, and M. Y. Li, "Active voltage control for DFIG-based wind farm integrated power system by coordinating active and reactive powers under wind speed variations," *IEEE Transactions on Energy Conversion*, vol. 34, no. 3, pp. 1504–1511, Sep. 2019.

[11] Y. F. Guo, H. L. Gao, D. Wang, and Q. W. Wu, "Online optimal feedback voltage control of wind farms: decentralized and asynchronous implementations," *IEEE Transactions on Sustainable Energy*, vol. 12, no. 2, pp. 1489–1492, Apr. 2021.

[12] Y. F. Guo, H. L. Gao, and Z. Y. Wang, "Distributed online voltage control for wind farms using generalized fast dual ascent," *IEEE Transactions on Power Systems*, vol. 35, no. 6, pp. 4505–4517, Nov. 2020.

[13] X. Yang, H. Zhao, and J. Zhang, "Distributed Cooperative Secondary Voltage Control in an Unbalanced Microgrid, " *CSEE Journal of Power and Energy Systems*, vol. 10, no. 1, pp. 222–234, Jan. 2024.

[14] Z. Li et al., "Tube Model Predictive Control Based Cyber-Attack-Resilient Optimal Voltage Control Strategy in Wind Farms "*CSEE Journal of Power and Energy Systems*, vol. 10, no. 2, pp. 530–538, Mar. 2024.

[15] R. Aghatehrani and R. Kavasseri, "Sensitivity-analysis-based sliding mode control for voltage regulation in microgrids," *IEEE Transactions on Sustainable Energy*, vol. 4, no. 1, pp. 50–57, Jan. 2013.

[16] S. Huang, Q. W. Wu, J. Zhao, and W. Liao, "Distributed optimal voltage control for VSC-HVDC connected large-scale wind farm cluster based on analytical target cascading method," *IEEE Transactions on Sustainable Energy*, vol. 11, no. 4, pp. 2152–2161, Oct. 2020.

[17] L. Guo, Y. X. Zhang, X. L. Li, Z. G. Wang, Y. X. Liu, L. Q. Bai, and C. S. Wang, "Data-driven power flow calculation method: a lifting dimension linear regression approach," *IEEE Transactions on Power Systems*, vol. 37, no. 3, pp. 1798–1808, May 2022.

[18] Y. X. Liu, N. Zhang, Y. Wang, J. W. Yang, and C. Q. Kang, "Data-driven power flow linearization: a regression approach," *IEEE Transactions on Smart Grid*, vol. 10, no. 3, pp. 2569–2580, May 2019.

[19] Y. X. Liu, Y. Wang, N. Zhang, D. Lu, and C. Q. Kang, "A data-driven approach to linearize power flow equations considering measurement noise," *IEEE Transactions on Smart Grid*, vol. 11, no. 3, pp. 2576–2587, May 2020.

[20] T. Xu, W. Wu, and F. Zhang, "Data-driven Inverter-based Volt/VAr Control for Partially Observable Distribution Networks, " *CSEE Journal of Power and Energy Systems*, vol. 9, no. 2, pp. 548–560, Mar. 2023.

[21] E. L. da Silva, A. M. N. Lima, M. B. de Rossiter Corrêa, M. A. Vitorino, and L. T Barbosa, "Data-driven sensitivity coefficients estimation for cooperative control of PV inverters," *IEEE Transactions on Power Delivery*, vol. 35, no. 1, pp. 278–287, Feb. 2020. .

[22] C. Andalib-Bin-Karim, X. D. Liang, N. Khan, and H. G. Zhang, "Determine Q-V characteristics of grid-connected wind farms for voltage control using a data-driven analytics approach," *IEEE Transactions on Industry Applications*, vol. 53, no. 5, pp. 4162–4175, Sep./Oct. 2017.

[23] J. H. Liu and J. S. Cheng, "Online voltage security enhancement using voltage sensitivity-based coherent reactive power control in multi-area wind power generation systems," *IEEE Transactions on Power Systems*, vol. 36, no. 3, pp. 2729–2732, May 2021.

[24] B. A. Robbins and A. D. Domínguez-García, "Optimal reactive power dispatch for voltage regulation in unbalanced distribution systems," *IEEE Transactions on Power Systems*, vol. 31, no. 4, pp. 2903–2913, Jul. 2016.

[25] Original data of training samples. [Online]. Available: https://docs.google.com/spreadsheets/d/1e0VaHHtpA_sGg0Lm3s3cbaZIibzZmI1B/edit?usp=sharing&ouid=108169409851494960527&rtpof=true&sd=true

Li Guo received the B.Sc. and Ph.D. degrees in Electrical Engineering from South China University of Technology in 2002 and 2007, respectively. He is currently a full Professor at Tianjin University. His research interests include the optimal planning and design of microgrid, the coordinated operating strategy of microgrid, and the advanced energy management system.

Zhaoning Liu received the B.Sc. degree from Hebei University of Technology, Tianjin, China, in 2021, the M.Sc. degree from Tianjin University, Tianjin, China, in 2021, both in Electrical Engineering. His current research interests include the modeling and optimization of power systems.

Zhongguan Wang received B.S. and Ph.D. degrees from the Department of Electrical Engineering, Tsinghua University, Beijing, China, in 2014 and 2019, respectively. He is currently an Associate Professor with the School of Electrical and Information Engineering, Tianjin University, Tianjin, China. His current research interests include operation of renewable power generation and active distribution system energy management.

Xialin Li received the B.Sc. degree and the Ph.D. degree from Tianjin University, Tianjin, China, in 2009 and 2014, respectively. Since 2014, he has been a Lecturer with the School of Electrical Engineering and Automation, Tianjin University, China. In 2016, under the State Scholarship Fund, he was invited as a Visiting Professor to the Department of Electrical and Computer Engineering, University of Alberta, Canada. His current research interests include the modeling and control of power converters, distributed generation, hybrid ac/dc microgrid, and multi-terminal dc grids (MTDC).

Yixin Liu received the B.S. and Ph.D. degrees in Electrical Engineering from Tianjin University, Tianjin, China, in 2013 and 2018, respectively. He is currently an Assistant Professor with Tianjin University. His research interests include the distribution system analysis and planning, energy management system of microgrid, and electricity power market.

Yuxuan Zhang received the B.Sc. degree from Northeast Electric Power University, Jilin, China, in 2018, the M.Sc. degree from Tianjin University, Tianjin, China, in 2021, both in Electrical Engineering. He is currently working toward the Ph.D. degree in Electrical Engineering at Tianjin University, Tianjin, China. His current research interests include the modeling and optimization of power systems.

Xiaodi Zang received the B.S. degree in Electrical Engineering from Harbin Institute of Technology, Harbin, China, in 2008. She is currently a Deputy General Manager of the Comprehensive Energy Division at CRRC Zhuzhou Electric Locomotive Research Institute Co., Ltd. Her research interests include grid connection technology for renewable power generation and energy storage technology.

Chengshan Wang received the Ph.D. degree in Electrical Engineering from Tianjin University, Tianjin, China, in 1991. From 1994 to 1996, he was a Senior Academic Visitor with Cornell University, Ithaca, NY, USA. From 2001 to 2002, he was a Visiting Professor with Carnegie Mellon University, Pittsburgh, PA, USA. He is currently a Professor with the School of Electrical Engineering and Automation, Tianjin University, where he is also the Director of the Key Laboratory of Smart Grid of Ministry of Education. His current research interests include distribution system analysis and planning, distributed generation system and micro-grid, and power system security analysis.